

based on silicon wire waveguides

Jingtao Zhou (周静涛)¹, Huajun Shen (中华军)¹, Rui Jia (贾锐)¹, Huanming Liu (刘焕明)¹,
Yidan Tang (汤益丹)¹, Chengyue Yang (杨成樾)¹, Chunlai Xue (薛春来)², and Xinyu Liu (刘新宇)^{1*}

¹Key Laboratory of Microelectronics Devices and Integrated Technology Institute of Microelectronics,
Chinese Academy of Sciences, Beijing 100029, China

²Institute of Semiconductors, Chinese Academy of Sciences, Beijing 100083, China

*Corresponding author: xyliu@ime.ac.cn

Received February 14, 2011; accepted March 25, 2011; posted online June 16, 2011

Two types of 1×2 multi-mode interference (MMI) splitters with splitting ratios of 85:15 and 72:28 are designed. On the basis of a numerical simulation, an optimal length of the MMI section is obtained. Subsequently, the devices are fabricated and tested. The footprints of the rectangular MMI regions are only 3×18.2 and 3×14.3 (μm). The minimum excess losses are 1.4 and 1.1 dB. The results of the test on the splitting ratios are consistent with designed values. The devices can be applied in ultra-compact photonic integrated circuits to realize the “tap” function.

OCIS codes: 230.1360, 230.7370, 230.7380.

doi: 10.3788/COL201109.082303.

Silicon-on-insulator (SOI)-based optical devices such as silicon wire waveguides^[1], photonic crystal waveguides^[2], and slot waveguides^[3], have recently become highly attractive devices for realizing ultra-compact photonic integrated circuits (PICs). Because of the ultrahigh index contrast between Si and SiO₂, silicon wire waveguides can confine light in small cross sections, and guide it with low loss through sharp bends, whose radii are only several microns. Thus, the optical functional devices based on silicon wire waveguides may have very small sizes. Multi-mode interference (MMI) splitters are one of the most important optical functional devices in PICs. They offer many advantages such as wide optical bandwidth, polarization independence, and large fabrication tolerance. These outstanding merits make them suitable for fabricating various optical devices such as beam splitters, couplers, and switches. MMIs based on silicon wire waveguides have been extensively investigated in recent years^[4]. The footprint of MMI devices may be as small as 3×9 (μm), and among all these devices, the 1×2 MMI is the simplest. An even splitting ratio of 50:50 is commonly used for light splitting and combining in PICs. In some particular applications, the 1×2 MMI with an uneven splitting ratio is necessary. In optical signal processing, for example, dividing the signal into two uneven parts is often required. The main branch is responsible for the transmission of the signal and the minor branch is responsible for monitoring the signal. This “tap” function is ordinarily used in ultra-compact PICs. For this application, three requirements are imposed on the 1×2 MMI: (1) compact size, (2) uneven splitting ratio, and (3) low excess loss (EL).

As mentioned above, the use of silicon wire waveguides for connection with input and output ports can endow MMI splitters with highly compact sizes. Through proper design based on the self-imaging principle, uneven splitting-ratio 1×2 MMI splitters with low EL can be realized. In this letter, two types of uneven splitting-ratio

1×2 MMI splitters based on silicon wire waveguides are designed. The splitters have splitting ratios of 85:15 and 72:28. The simulation tool BeamPROP (Rsoft) is used to analyze coupling efficiency and optimize device performance. On the basis of a numerical simulation, an optimal length of the MMI section is obtained for fixing the thickness of the core layer and the width of the MMI waveguides. Subsequently, the 1×2 MMI splitters are fabricated and tested. The performance of the devices is discussed in comparison with the simulation result.

The operation of a MMI device is based on the so-called self-imaging principle. An analytical theory that provides the positions, amplitudes, and phases of the self-images in $N \times N$ MMI couplers has been reported^[5]. N self-images of equal intensities $1/N$ are formed at the output of MMI couplers of length L_N^M , expressed as

$$L_N^M = \frac{3M}{N} L_c, \quad (1)$$

where M and N are any positive integers without a common divisor. To obtain a compact size, $M = 1$ is required for short MMI couplers. L_c is the coupling length between the two lowest order modes. With strongly guided eigenmodes in the MMI section and paraxial approximation for the propagation constants, L_c can be written as

$$L_c \approx \frac{4n_r W^2}{3\lambda}, \quad (2)$$

where n_r represents the effective index of the MMI waveguide, the working wavelength $\lambda = 1.55$ μm , and W is the width of the MMI waveguide. If the positions of input and output ports satisfy the equation

$$x_i^{\text{in}} = \frac{W}{N} i, \quad i = 1, 2, 3, \dots, N - 1, \quad (3)$$

an overlapping-image MMI coupler is formed. Because previously separated images merge in pairs, a reduced

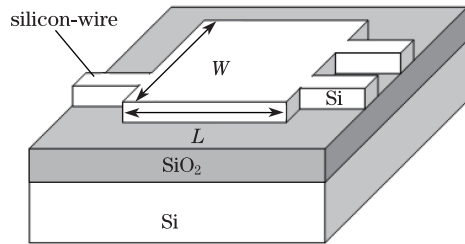


Fig. 1. Schematic of the uneven splitting-ratio 1×2 MMI splitters.

Table 1. Overlapping-Image MMI Splitters with Nonuniform Splitting Ratios of 85:15 and 72:28

Splitting Ratio	N	Input Position	Output Position	Length ($L = \frac{3L_c}{N}$)
85:15	4	$\frac{W}{4}$	$\frac{W}{4}, \frac{3W}{4}$	$\frac{3L_c}{4}$
72:28	5	$\frac{W}{5}, \frac{3W}{5}$	$\frac{2W}{5}, \frac{4W}{5}$	$\frac{3L_c}{5}$

number of images can be obtained. An overlapping-image MMI produces non-uniform power distributions. For $N \leq 12$, all possible input and output positions in overlapping-image MMI couplers are listed^[6]. Among all the overlapping-image MMI couplers, we are mostly concerned with the 1×2 MMI splitter. Four splitting ratios (100:0, 85:15, 72:28, and 50:50) can be realized. Given that the 1×2 MMI splitters with splitting ratios of 50:50 and 100:0 are unsuitable for the ‘‘tap’’ application, we focus on the 1×2 MMI splitters with splitting ratios of 85:15 and 72:28. The input and output positions, as well as the lengths of the MMIs are shown in Table 1.

The simulation was conducted using a three-dimensional beam propagation method (3D-BPM) (Rsoft BeamPROP) to optimize the property of the MMI splitters. The schematic configuration of the 1×2 MMI splitters for the simulation is shown in Fig. 1. All the optical devices are based on a SOI wafer with a silicon core thickness of $0.26 \mu\text{m}$ and a $1\text{-}\mu\text{m}$ buried oxide layer. Thus, the waveguide height chosen is $0.26 \mu\text{m}$. To minimize the footprint of the MMI splitters, the width of MMI region W should be as small as possible, according to Eq. (2). Conversely, W cannot be excessively reduced because the multimode waveguide must be designed to support a large number of transverse modes (typically >3)^[5]. Although the device may be more compact, the narrow gap between the input and output waveguides may cause signal crosstalk and even make the fabrication difficult. We have ascertained that the MMIs not only have compact sizes but also support a sufficient number of transverse modes when the width chosen is $3 \mu\text{m}$ ^[4]. The effective index n_r of the MMI waveguides is calculated to be 2.968. The width of the silicon wire waveguide connected to the input and output ports is $0.5 \mu\text{m}$, which satisfies the mono-mode transmission condition. When we substitute all the factors in Eq. (1), the length of the MMI couplers L can be calculated as

$$L_1 = 17.3 \mu\text{m} \text{ (for 85 : 15), } L_2 = 13.8 \mu\text{m} \text{ (for 72 : 28).}$$

We set a transparent boundary condition to simulate the field propagation in the MMI coupler. The grid sizes are set as $\Delta x = \Delta y = 0.005 \mu\text{m}$ and $\Delta z = 0.01 \mu\text{m}$. Figure 2 shows the normalized total powers and the splitting ratios at different lengths of the MMI waveguide with an ideal splitting ratio of 85:15. Here, the splitting ratio is defined as the percentage of the total optical power in the main branch of the two output ports. The figure shows that a maximum total optical power of 0.892 and a splitting ratio of 88% can be obtained at $17.9 \mu\text{m}$. According to the designed splitting ratio of 85%, the corresponding length of the MMI should be $18.3 \mu\text{m}$. To obtain an exact splitting ratio and low EL at the same time, a tradeoff is made in choosing the length $18.2 \mu\text{m}$. A splitting ratio of 85.6% and an output power of 0.874 are obtained. Thus, the corresponding EL is 0.58 dB.

Figure 3 shows the normalized total powers and the splitting ratios at different lengths of the MMI waveguide with the ideal splitting ratio of 72:28. It shows that a maximum total output power of 0.929 and a splitting ratio of 72.5% can be obtained at $14.3 \mu\text{m}$. Because the splitting ratio is highly consistent with the ideal value of 72:28, an optimized MMI length of $14.3 \mu\text{m}$ is obtained. The corresponding EL is only 0.32 dB.

Using electron beam lithography and inductively coupled plasma etching, we accurately fabricated 1×2 MMI splitters with splitting ratios of 85:15 and 72:28. The

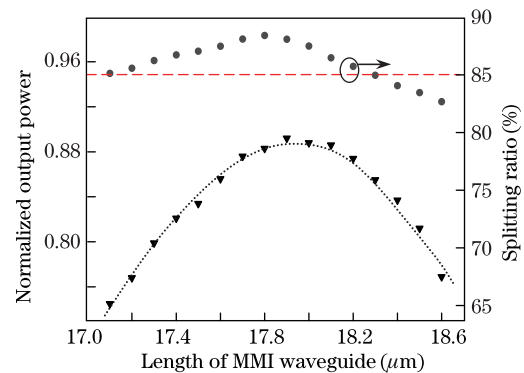


Fig. 2. Normalized total powers and splitting ratios at different lengths of the MMI waveguide with the ideal splitting ratio of 85:15.

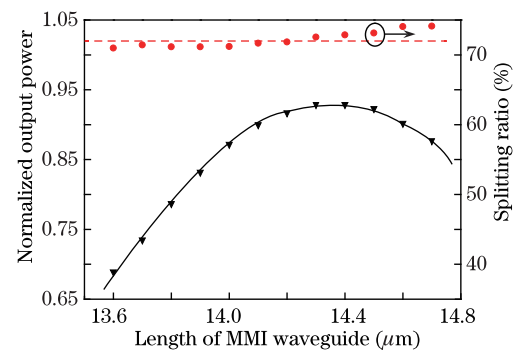


Fig. 3. Normalized total powers and splitting ratios at different lengths of the MMI waveguide with the ideal splitting ratio of 72:28.

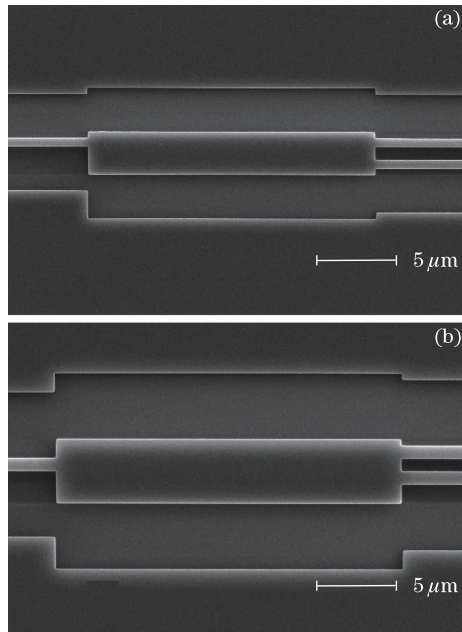


Fig. 4. SEM images of the 2×2 MMI couplers with (a) 85:15 and (b) 72:28 splitting ratios.

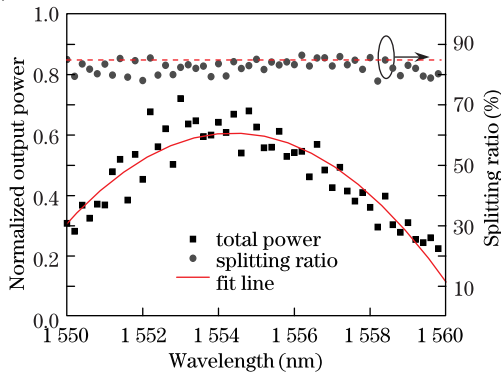


Fig. 5. ELs and actual splitting ratios of the 1×2 MMI splitter with the splitting ratio of 85:15.

scanning electronic microscopy (SEM) images of the devices are shown in Fig. 4. The footprints of the rectangular MMI regions are only 3×18.2 and 3×14.3 (μm), respectively.

Figure 5 shows the EL and actual splitting ratios of the 1×2 MMI splitters with splitting ratio of 85:15, which are in the range of 1550–1560 nm. The splitters were calibrated using neighboring simple silicon wires with the same lengths. Figure 5 also shows that the average EL of the 1×2 MMI splitter with the splitting ratio of 85:15 is 3.2 dB. The minimum EL is 1.4 dB at a wavelength of 1553 nm. The splitting ratio varies in the range of 78%–86%. The average value of 83.5% is obtained.

In Fig. 6, we can see that the average EL of the 1×2 MMI coupler with the splitting ratio of 72:28 is 2.8 dB. The minimum EL is 1.1 dB at a wavelength of 1,556 nm. The splitting ratio varies in the range of 65%–75%. The average value of 70.2% is obtained.

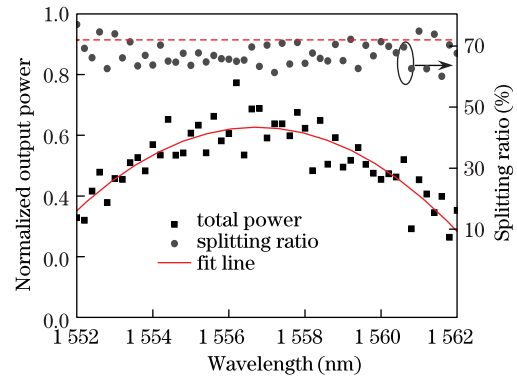


Fig. 6. ELs and actual splitting ratios of the 1×2 MMI splitter with the splitting ratio of 72:28.

The devices exhibit a consistency with the simulation results. The ELs are comparatively low and the splitting ratios approximate the design value within $\pm 5\%$ at a wavelength range of more than 10-nm wide. The uncertainty during the test and imperfections in the fabrication cause a slight deviation from the simulation results. Strict and accurate control in the fabrication process is needed to improve the performance of the devices.

In conclusion, two types of uneven splitting-ratio 1×2 MMI splitters based on silicon wire waveguides are designed and fabricated. The simulation results show the optimized length of the MMI regions for the two devices. The devices exhibit a consistency with the simulation results. The footprints of the rectangular MMI regions are only 3×18.2 and 3×14.3 (μm), respectively. The minimum ELs are 1.4 and 1.1 dB. The results of the test on the splitting ratios are consistent with the designed values. On the basis of compact size, low EL, and uneven splitting ratios, we conclude that the devices can be applied in ultra-compact PICs to realize the tap function in optical signal processing.

This work was supported in part by the National Natural Science Foundation of China (No. 60977050) and the National “973” Program of China (Nos. 2009CB320302 and 2011CB301704).

References

1. Y. Vlasov and S. McNab, *Opt. Express* **12**, 1622 (2004).
2. Y. Huang, X. Mao, C. Zhang, L. Cao, K. Cui, W. Zhang, and J. Peng, *Chin. Opt. Lett.* **6**, 704 (2008).
3. A. E. Willner, L. Zhang, Y. Yue, and X. Wu, *Chin. Opt. Lett.* **8**, 909 (2010).
4. J. Zhou, H. Shen, H. Zhang, and X. Liu, *Chin. Opt. Lett.* **7**, 1041 (2009).
5. L. B. Soldano and E. C. M. Pennings, *J. Lightwave Technol.* **3**, 615 (1995).
6. M. Bachmann, P. A. Besse, and H. Melchior, *Appl. Opt.* **34**, 6898 (1995).